# Supplementary Information

## Synergistic Protein-reinforced DNA Hydrogels with Tunable Biomechanics for Mechanoresponsive Drug Release

*Kanchan Yadav†[a], Iksoo Jang†[a], Yoonbin Ji[a], Taehyeon Kim[a], Peter Chang-Whan Lee*[cd], Jong Bum Lee*[ab]*

[a]Chemical Engineering Department, University of Seoul, Seoul-02504, Republic of Korea

[b]Center for Innovative Chemical Processes, Institute of Engineering, University of Seoul, 163 Seoulsiripdaero, Dongdaemun-gu, Seoul 02504, Republic of Korea.

[c]Department of Biochemistry & Molecular Biology, College of Medicine, University of Ulsan, Asan Medical Center, Seoul, 05505, Republic of Korea

[d]Lung Cancer Research Center, Asan Medical Center, University of Ulsan College of Medicine, Seoul, 05505, Republic of Korea

* Corresponding author:

Correspondence to Jong Bum Lee, Peter Chang-Whan Lee

* Peter C. W. Lee, PhD, Department of Biochemistry & Molecular Biology, University of Ulsan College of Medicine, Asan Medical Center, Seoul, 05505, Republic of Korea. E-mail: pclee@amc.seoul.kr

* Jong Bum Lee, PhD, Department of Chemical Engineering, University of Seoul, 163 Seoulsiripdaero, Dongdaemun-gu, Seoul, 02504, Republic of Korea. E-mail: jblee@uos.ac.kr

Email: Kanchany10038@gmail.com, iksoojang.uos@gmail.com , Yoonbinji.uos@gmail.com, thkimuosuos@gmail.com

*†: equal contribution*

**Supplementary Tables and Figures**

**Table S1.** List of DNA and multiprimer sequences used to form BRIDGe

| Name | Sequence (5'-3') |
|---|---|
| Linear DNA | 5’-Phosphate-TCG TTT GAT GTT CCT AAC GTA CCA ACG CAC ACG CAG TAT TAT GGA CTG GTA AAA GCT TTC CGA GGT AGC CTG GAG CAT AGA GGC ATT GGC TG-3’ |
| Primer for circular DNA | 5’-TAG GAA CAT CAA ACG ACA GCC A-3’ |
| Multiprimer1 | 5’-ACG CAG TAT TAT GGA CTG-3’ |
| Multiprimer2 | 5’-TGG TAC GTT AGG AAC ATC-3’ |

**Table S2.** List of various linear templates of DNA to justify the applicabilty of protein reinformacemnt process to form BRIDGe

| Name | Sequence (5'-3') |
|---|---|
| BRIDGe Linear DNA | 5’-Phosphate-TCG TTT GAT GTT CCT AAC GTA CCA ACG CAC ACG CAG TAT GGA CTG GTA AAA GCT TTC CGA GGT AGC CTG GAG CAT AGA GGC ATT G G-3’ |
| CpG linear DNA | 5’-Phosphate –TAG TTT CAT GTT TGG CTA CTC TAC TTA GAT TAA CGT CAG GAA CGT CAT GGA CTG AGT ACT TAG ATT AAC GTC AGG AAC GTC ATG GAG GAA TG-3’ |
| IBA linear DNA | 5’-Phosphate –AGG GAT ATG CCT CTA ATA AAT ATT AAC CAG AAG ACA C CC TAC CAA CCC CCC CCA CCA CCA TAA GAA GTT GGT ACG TTA ATA CG A CTC ACT AT-3’ |

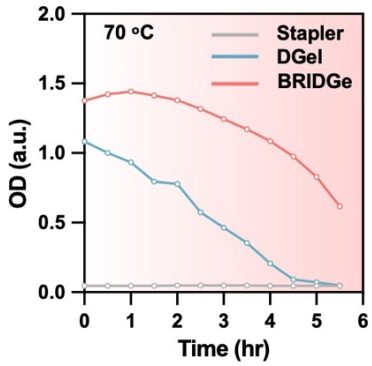


**Figure S1.** Comparative changes in optical density of BRIDGe, DGel, and stapler (BSA) during gelation under prolonged incubation at 70 °C.

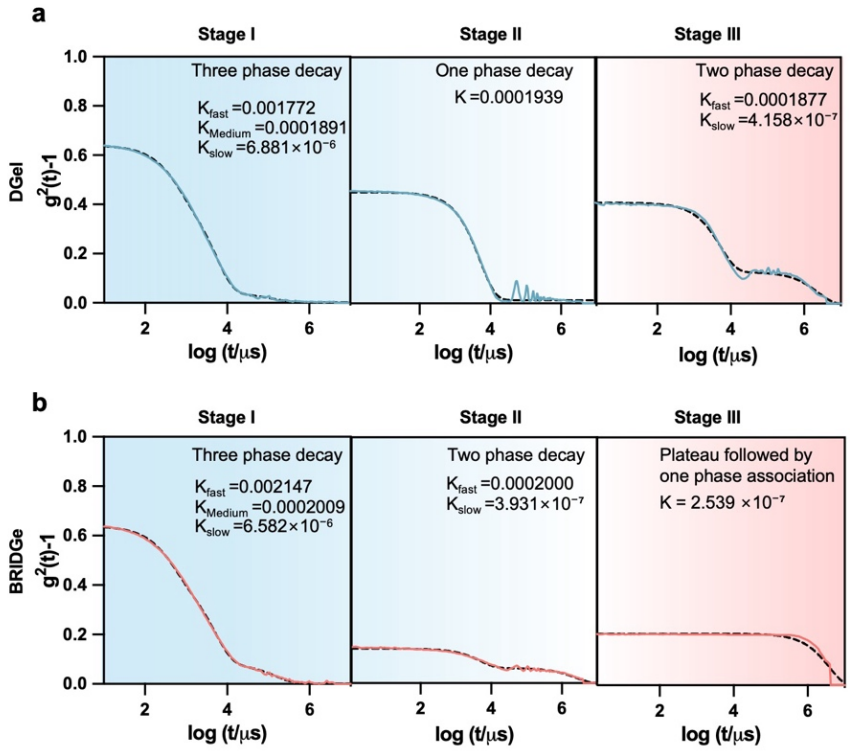


**Figure S2.** DLS autocorrelation functions of (a) DGel and (b) BRIDGe hydrogels measured at phase transition points: pregel state I _ 6 h, soft gel state II _ 20 h, after stapling process state III _ 21 h.

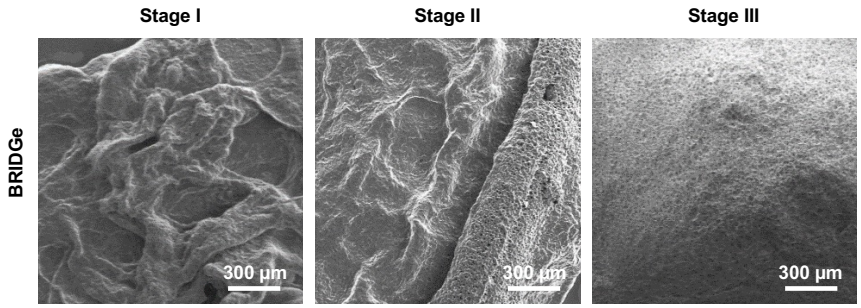


**Figure S3.** SEM images of BRIDGe at phase transition points: pregel state I _ 6 h, soft gel state II _ 20 h, after stapling process state III _ 21 h.

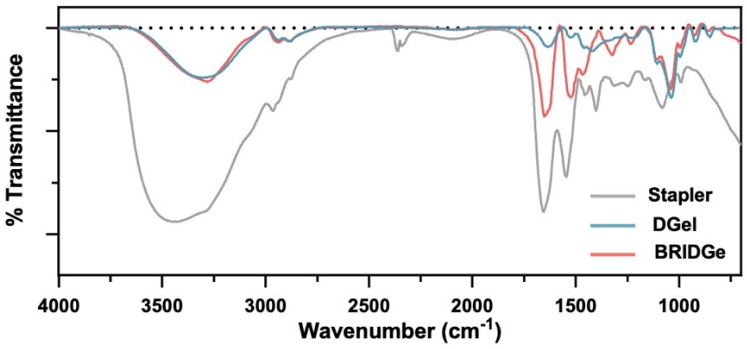


**Figure S4.** Comparative full-scan FTIR spectra of BRIDGe, DGel, and stapler (BSA protein)

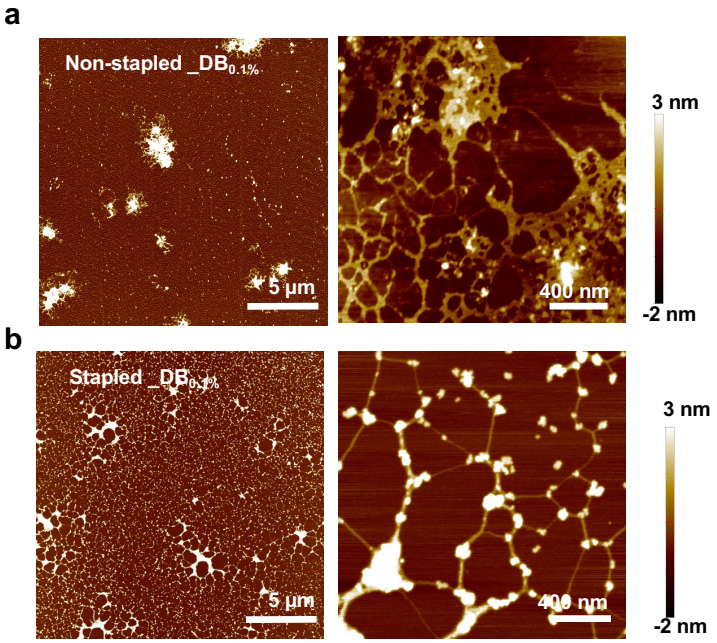


**Figure S5.** AFM images of (a) non-stapled and (b) stapled hydrogel (heating at 70 °C _ 1 h) at an early stage of RCA (4 h) with a lower concentration of the BSA protein (1 mg/ml).

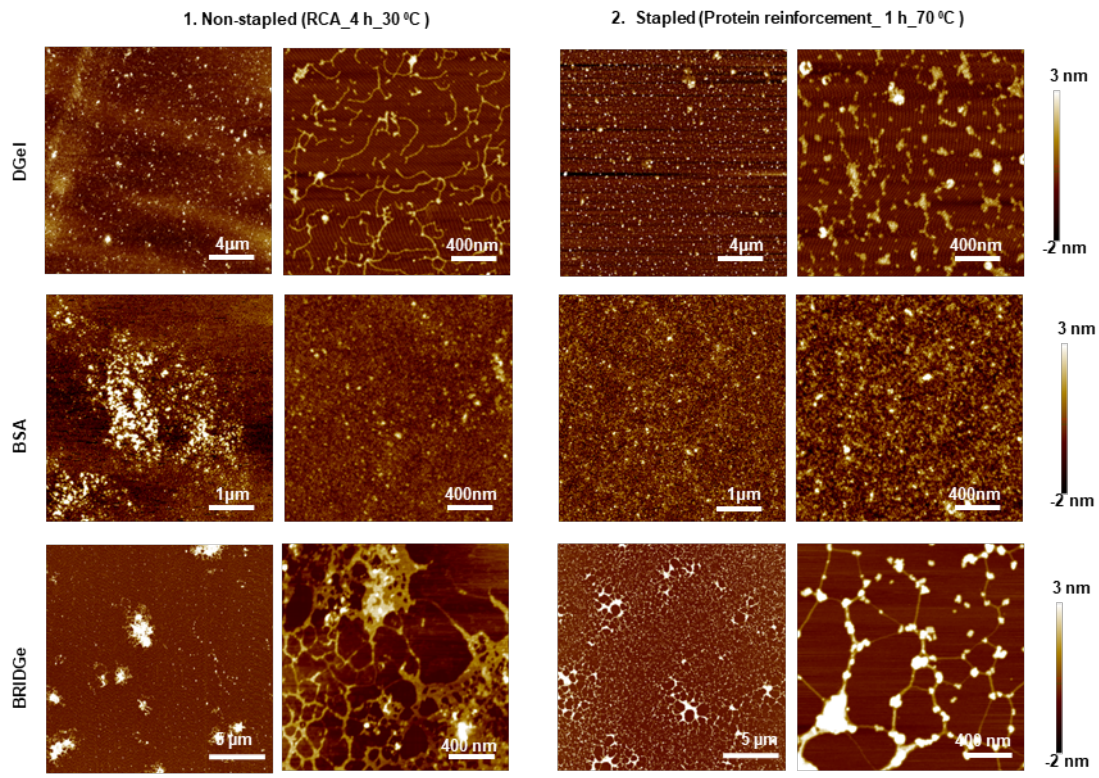


**Figure S6**. AFM images of Dgel, BSA and BRIDGe with and without stapling process (heating at 70 °C) at early stage of RCA (4 h) and lower concentration of the BSA (1mg/ml).

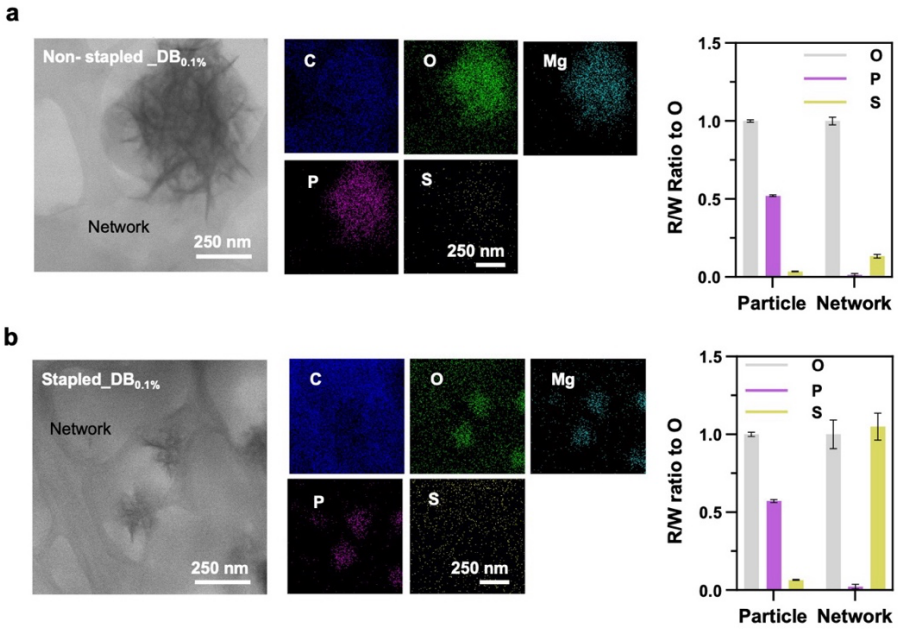


**Figure S7.** TEM images of (a) non-stapled and (b) stapled hydrogels, with EDS elemental mapping of carbon (C; blue), oxygen (O; green), magnesium (Mg; cyan), phosphorus (P; violet), and sulfur (S; yellow). The attached bar graphs (top: non-stapled hydrogel, bottom: stapled hydrogel) show the relative weight ratio of phosphorus and sulfur at particle and connecting network sites compared to oxygen.

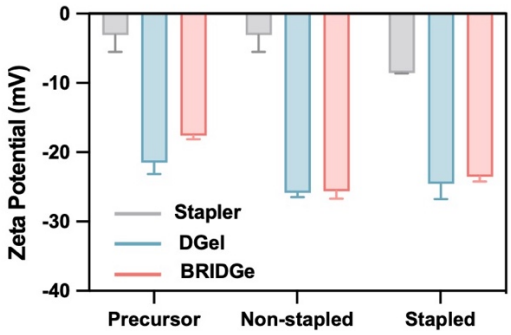


**Figure S8**. Zeta potential measurements were performed for the precursor solution, DGel, and BRIDGe formulations with and without the stapling process (heating at 70 °C), under conditions corresponding to the early stage of RCA reaction (4 h) and a lower BSA concentration (1 mg/mL).

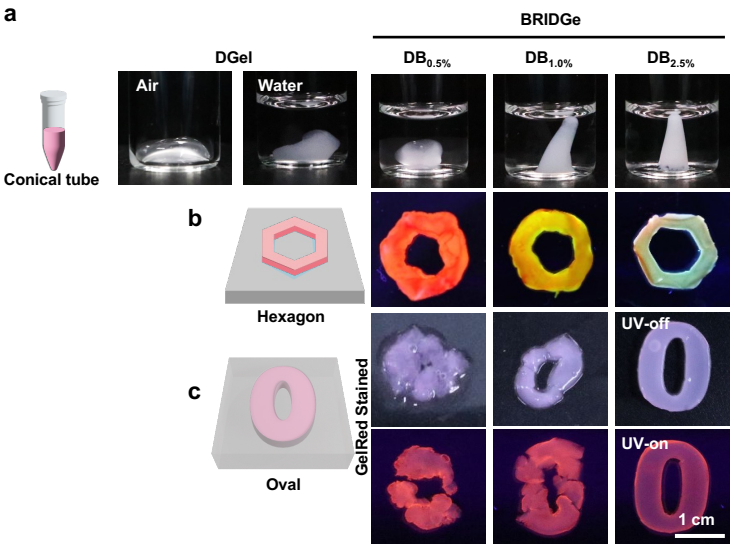


**Figure S9.** Digital images of DGel and stapled hydrogels ($DB_{0.5\%}$, $DB_{1.0\%}$, and $DB_{2.5\%}$) in various molds (a. conical tube, b. Hexagon shape PDMS mold, c. oval-shaped PDMS mold) to demonstrate the versatile applicability of the hydrogels for various biomedical implants. Additionally, GelRed-stained hydrogel images under UV light show the homogeneous integration of DNA in the stapled hydrogel network.

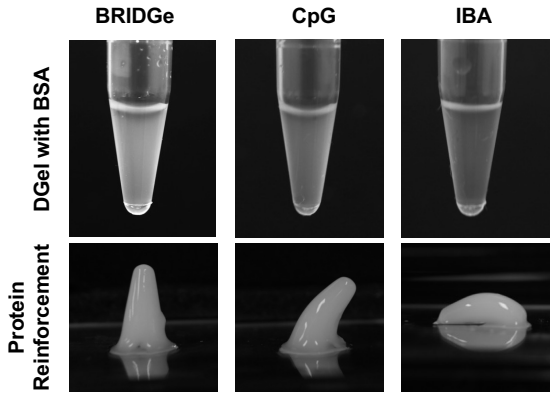


**Figure S10**. Digital images of the protein-reinforced hydrogels prepared with various DNA sequences demonstrate the versatility of the two-step gelation process.

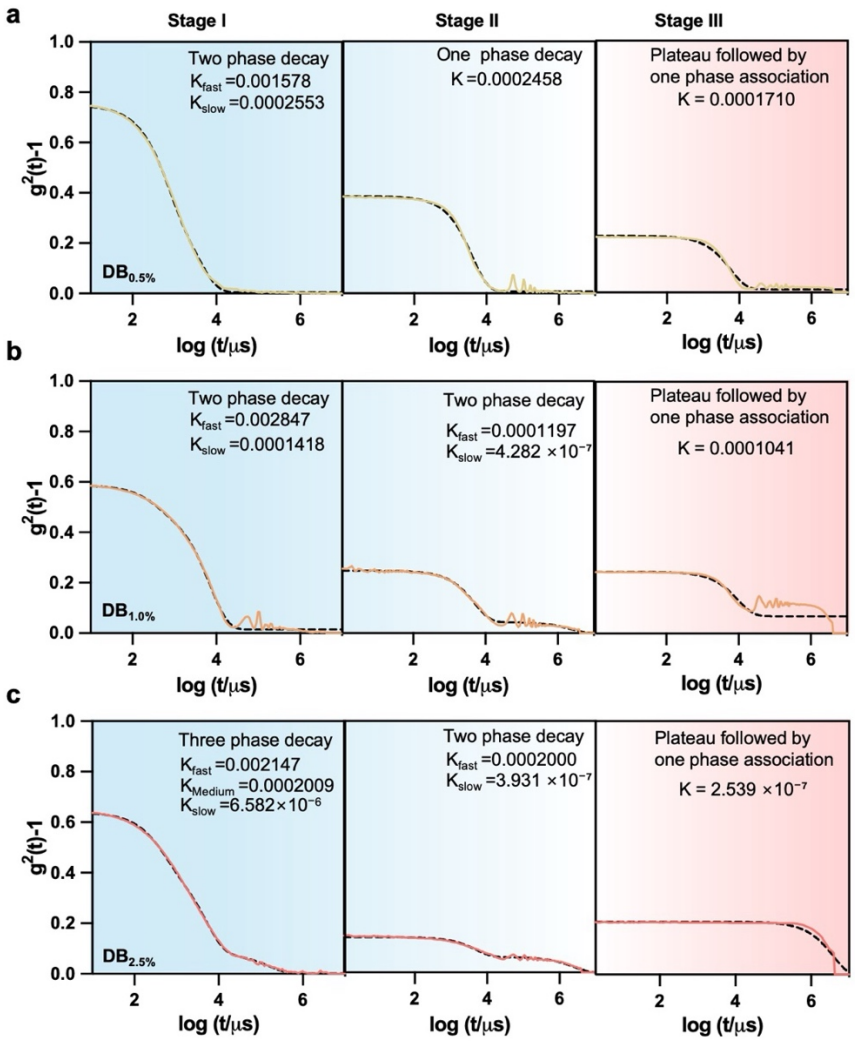


**Figure S11.** Comparative DLS autocorrelation function of (a) $DB_{0.5\%}$, (b) $DB_{1.0\%}$, and (c) $DB_{2.5\%}$ hydrogels at phase transition points: pregel: state I _ 6 h, soft gel: state II _ 20 h, after stapling process: state III _ 21 h.

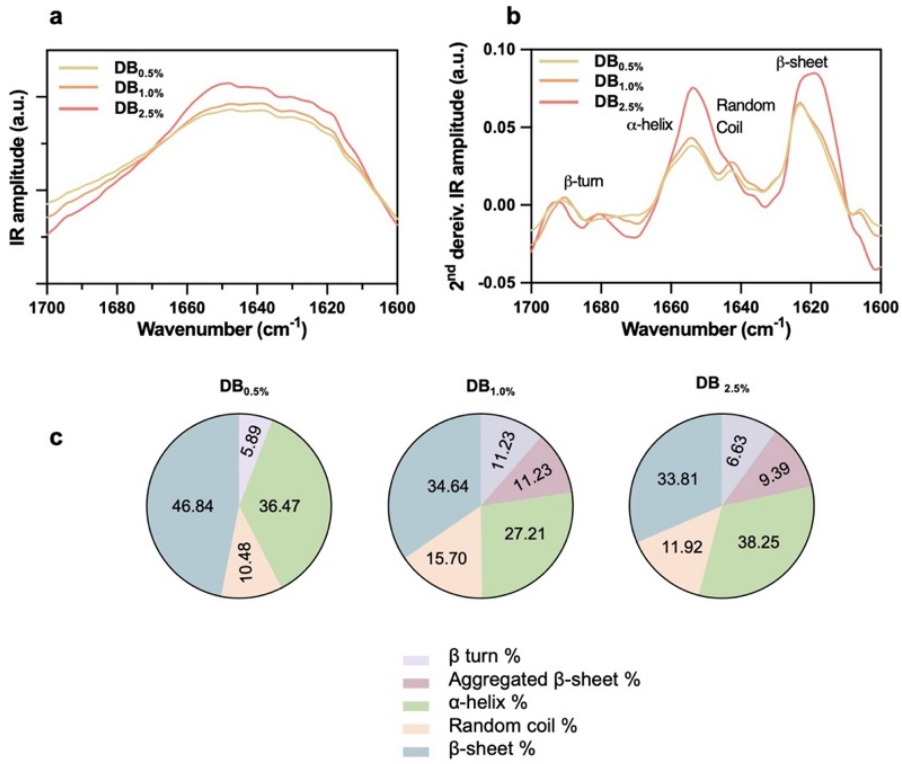


**Figure S12.** (a) FTIR spectra of stapled hydrogels in the amide I region (1700–1600 $cm^{-1}$). (b) Second-derivative IR analysis to understand the transformation of secondary structures with increasing percentage of stapling. (c) Pie charts showing the percentage of each secondary structure in stapled hydrogels with increasing percentage of BSA protein.

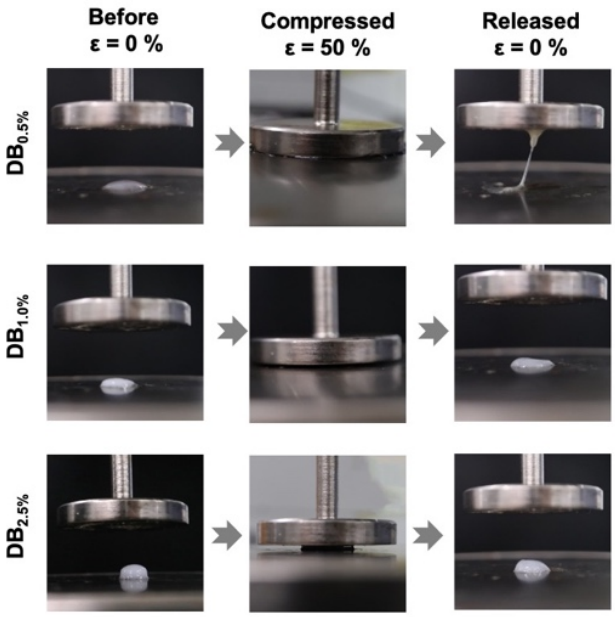


**Figure S13.** Stapled hydrogels ($DB_{0.5\%}$, $DB_{1.0\%}$, and $DB_{2.5\%}$) under 50% compressive strain.

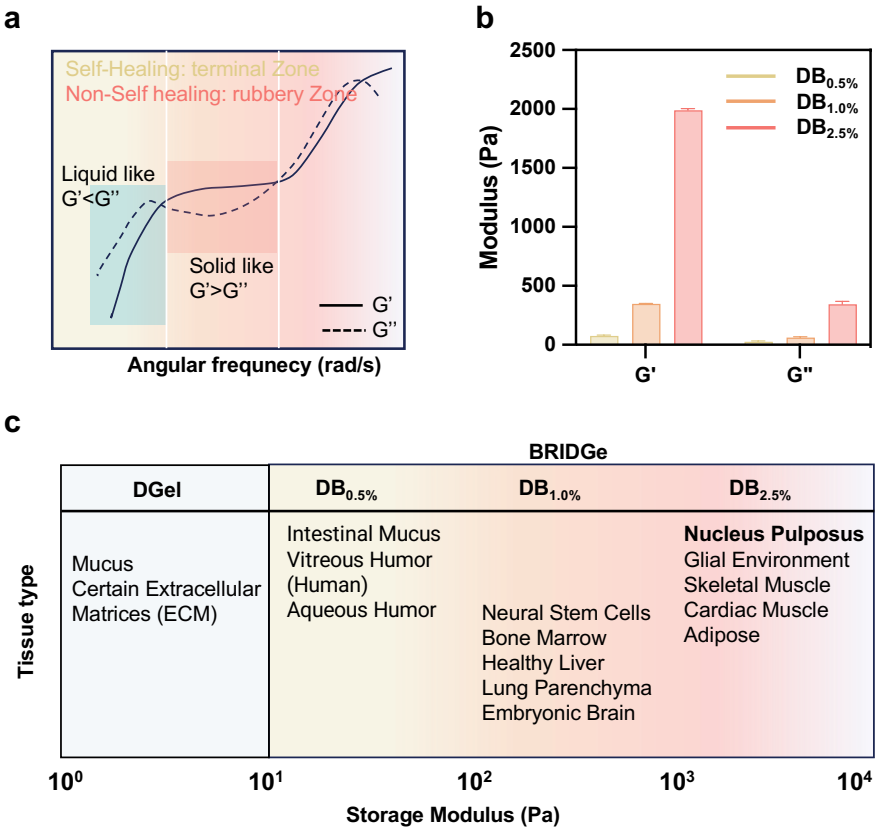


**Figure S14.** (a) Model spectra for angular-frequency-dependent physical states of hydrogel. (b) Comparative analysis of storage modulus (G') and loss modulus (G") of hydrogels at a frequency of 1 rad/s. (c) Coherence between tunable BRIDGe hydrogels and native soft tissues based on storage modulus. The stiffness range of BRIDGe hydrogels ($DB_{0.5\%}$, $DB_{1.0\%}$, $DB_{2.5\%}$) spans approximately 1–10 kPa, aligning with the mechanical properties of nucleus pulposus tissue and other biological tissues.

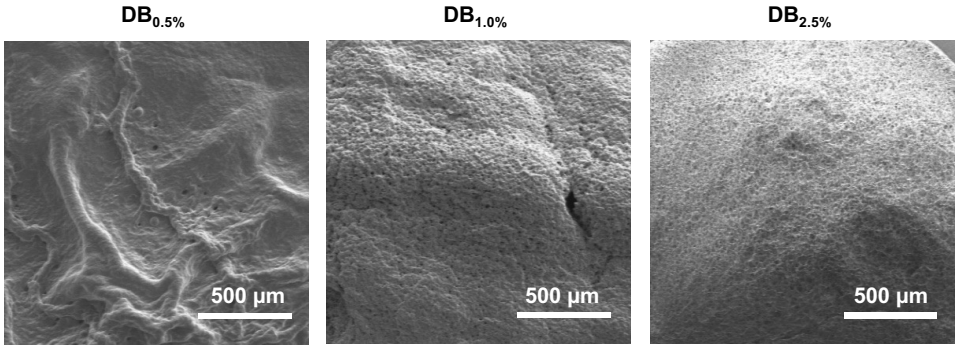


**Figure S15.** SEM images of stapled hydrogels $DB_{0.5\%}$, $DB_{1.0\%}$, and $DB_{2.5\%}$.

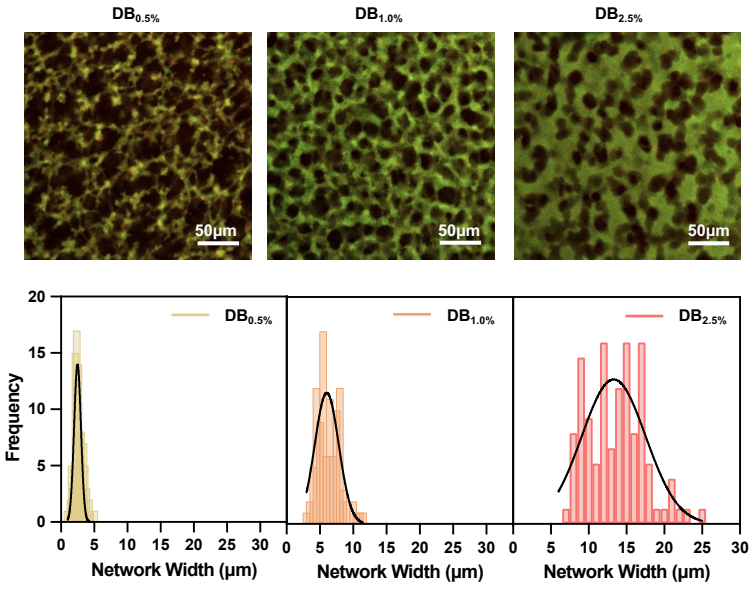


**Figure S16.** CLSM images of stapled hydrogels ($DB_{0.5\%}$, $DB_{1.0\%}$, and $DB_{2.5\%}$) and respective network width distribution histograms.

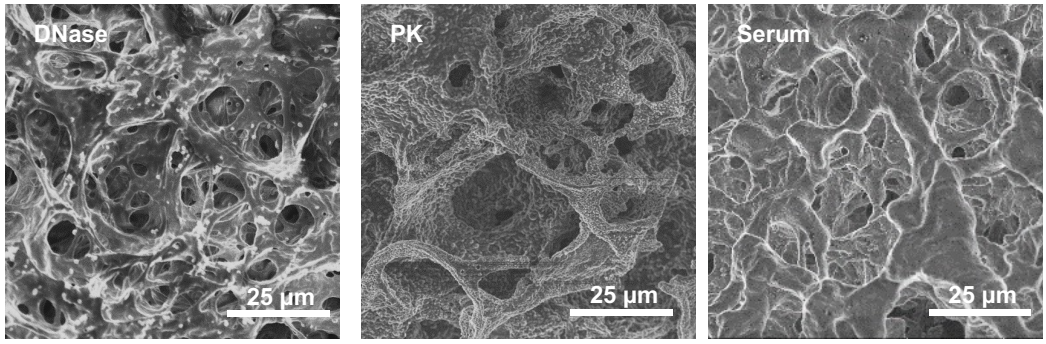


**Figure S17.** Physical states of $DB_{2.5\%}$ hydrogel in various enzymatic conditions: DNase, Proteinase K (PK), and serum.

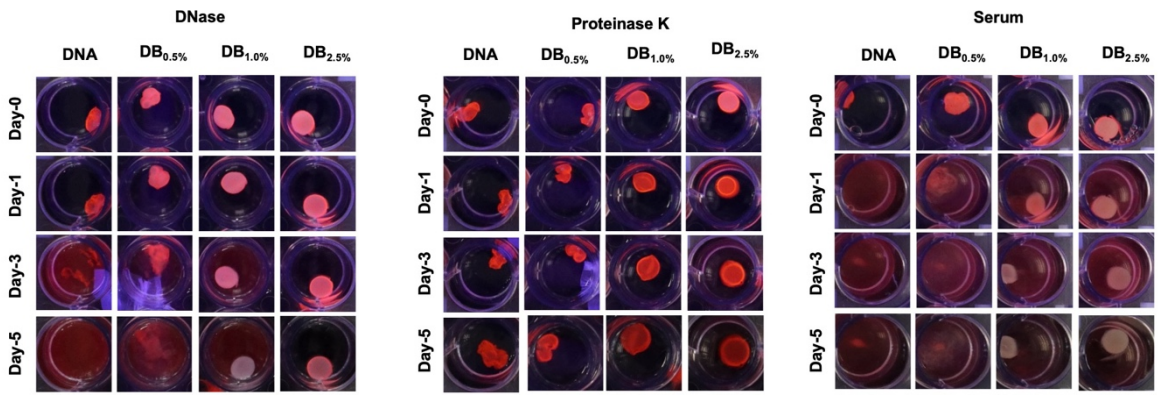


**Figure S18.** Stability analysis of stapled hydrogels in various enzymatic conditions over a period of 5 days.

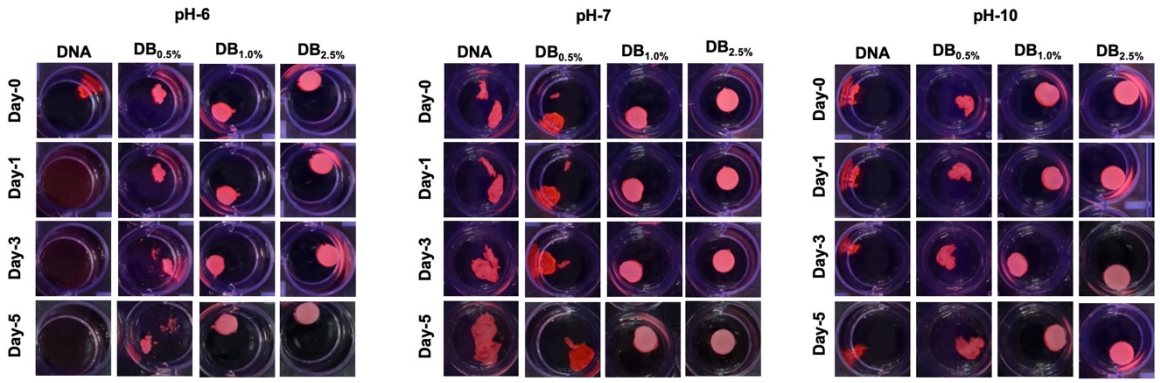


**Figure S19.** Stability analysis of stapled hydrogels in various pH conditions over a period of 5 days.

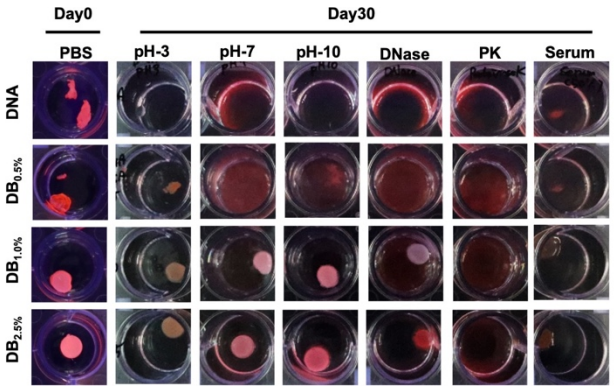


**Figure S20.** Comparative analysis of stapled hydrogels in various enzymatic and pH conditions over a period of 30 days.

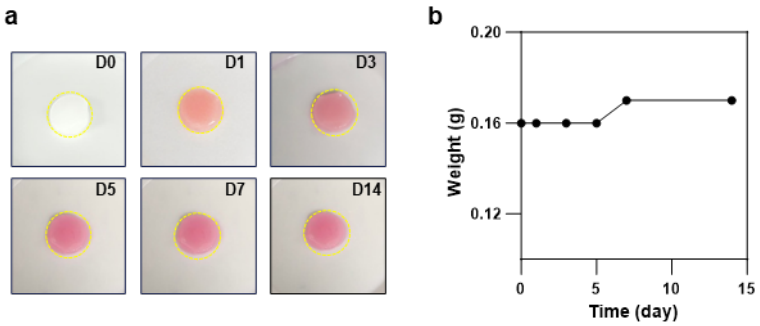


**Figure S21**. Stability analysis of BRIDGe in high concentration of pro-inflammatory cytokines serum. (a) Digital image of BRIDGe during a 14-day incubation period (D0-D14) in serum containing pro-inflammatory cytokines. (b) Time dependent wight profile of BRIDGe over 14 days.

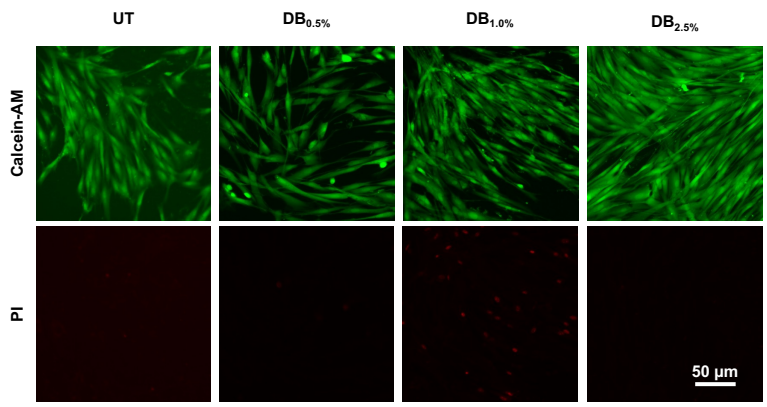


**Figure S22.** Fluorescence image of live and dead cells: living cells show green fluorescence (Calcein-AM), and dead cells emit red fluorescence from propidium iodide (PI).

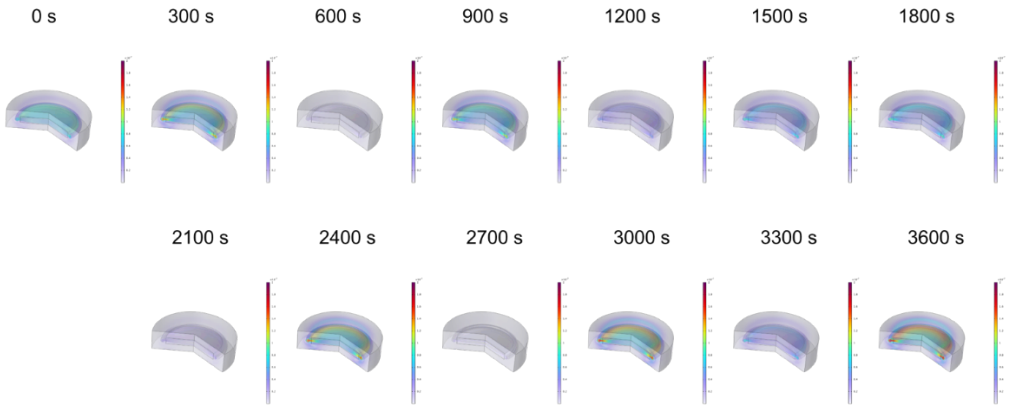


**Figure S23**. COMSOL finite element analysis of the hydrogel under repetitive compressive loading. Time-lapse simulation profiles tracking the spatial distribution of internal von Mises stress within the DB2.5% hydrogel disk during continuous cyclic compressive loading for 3600 s (1 h). The color-coded scale indicates the magnitude and redistribution of mechanical stress.

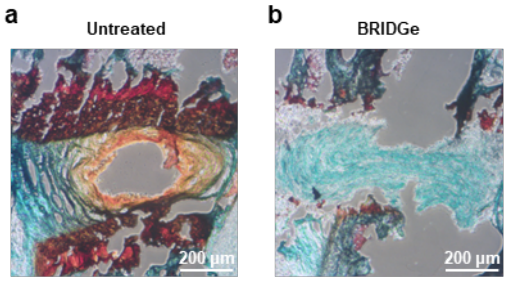


**Figure S24**. Ex-vivo structural stability and interface conformity of the BRIDGe . Safranin-O / Fast Green staining of mouse spines at Day 5 post-surgery in organ culture. (a) Intact normal control (UT) showing a well-organized, GAG-rich disc matrix (red). (b) BRIDGe group 5 days post-discectomy.

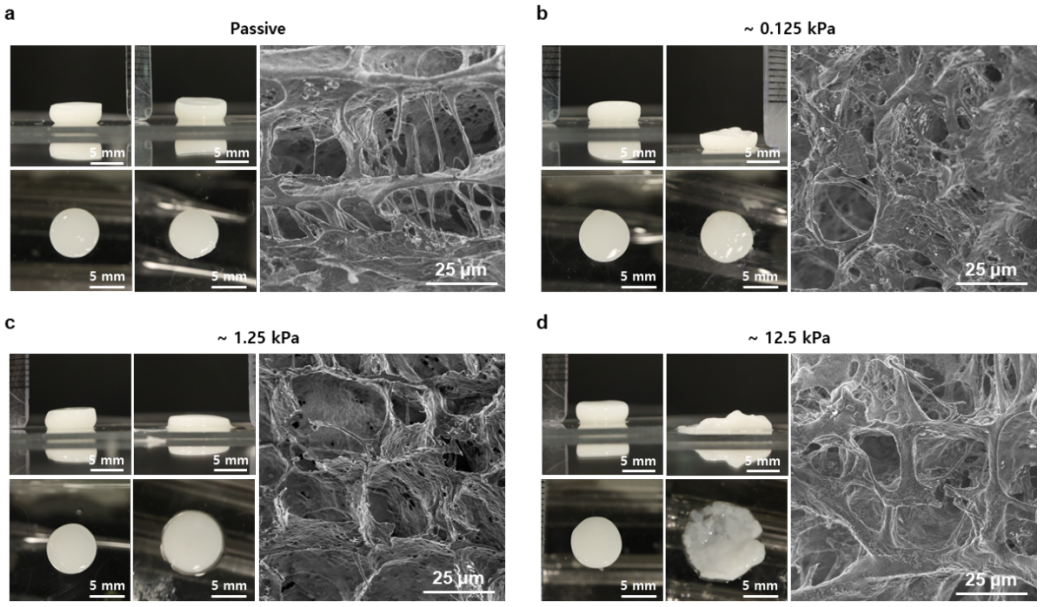


**Figure S25**. Digital images (top and side views) and scanning electron microscopy (SEM) images of the hydrogels after continuous application of mechanical forces for 1 h: (A) no stimulus, (B) 0.125 kPa, (C) 1.25 kPa, and (D) 12.5 kPa. Scale bars represent 5 mm for digital images and 25 µm for SEM images.